4.4 MODEL AEROSOL SENSITIVITY STUDIES AND MICROPHYSICAL INTERACTIONS IN AN OROGRAPHIC SNOWFALL EVENT

Stephen M. Saleeby[1]*, Randolph D. Borys[2], Melanie A. Wetzel[2], Dave Simeral[2], Michael P. Meyers[3], William R. Cotton[1], Ray McAnelly[1], N. Larson[3], and E. Heffernan[3]

[1]*Department of Atmospheric Science, Colorado State University, Fort Collins, CO*
[2]*Storm Peak Laboratory, Division of Atmospheric Sciences, Desert Research Institute, Reno, NV*
[3]*National Weather Service, Grand Junction, CO*

1. INTRODUCTION

Orographically enhanced snowfall events are common occurrences along the north/south oriented Park Range of North Central Colorado during the winter months. Within this mountain range, The Desert Research Institute operates Storm Peak Laboratory (SPL), a high-altitude atmospheric physics lab located at the summit of Mt. Werner (~3210m MSL) near Steamboat Springs, Colorado (Borys and Wetzel, 1997). A strong cross-barrier pressure gradient and resulting westerly upslope wind tends to frequently produce an orographic cloud with supercooled liquid water over SPL (Rauber and Grant, 1986; Borys et al., 2000).

A seeder-feeder mechanism, involving the sedimentation of higher altitude snow crystals through the low-level orographic cloud, produces greater precipitation amounts near mountaintop due to ample riming of cloud droplets in the lowest 2km (Rauber et al., 1986; Reinking et al., 2000). This low-level riming process enhances the precipitation efficiency, such that, the amount of rime has been shown to comprise from 20% - 50% of the final snow mass that reaches the surface (Mitchell et al., 1990; Borys et al., 2003).

Enhanced riming will increase the mass of snow crystals as well as the fall speed; this increases the likelihood of higher snow deposits along windward slopes (Hindman, 1986). Slower falling, unrimed snow crystals are more likely to fall on the leeward slopes where subsidence leads to evaporation, a reduction in total surface snowfall, and disappearance of the “feeder” cloud (Rauber et al., 1986; Rauber and Grant, 1986). Dry-season water supplies in Colorado rely strongly on the winter snow-pack, which is quite dependent upon riming to enhance precipitation efficiency.

Characteristics of the cloud droplet spectra in the orographic cloud directly impact the riming efficiency. Aerosol concentrations, primarily those with the composition to act as cloud condensation nuclei (CCN), will determine the droplet size and number concentration, and thus, the ice particle riming efficiencies (Hindman, 1994). Borys et al. (2000) found that increased sulfate-based aerosol concentrations suppress formation of larger cloud droplets and reduce riming of cloud droplets by ice hydrometeors.

Corresponding author address: Stephen M. Saleeby, Colorado State Univ., Atmos. Sci. Dept., Fort Collins, CO 80523; e-mail: smsaleeb@atmos.colostate.edu

Pruppacher and Klett (1997) delineate 10μm to be the cloud droplet riming cut-off diameter below which riming efficiencies are near zero.

This study seeks to examine the impact of aerosol concentration upon cloud droplet spectra, the riming growth process, and orographic snowfall along the Park Range, including SPL. This is accomplished with use of a mesoscale model to produce high resolution simulations of a winter orographic snowfall event that impacted SPL from Feb 7 – 9, 2005.

2. MODEL DESCRIPTION

The Colorado State University - Regional Atmospheric Modeling System (RAMS) Version 4.3 has been utilized for a set of sensitivity simulations with varying amounts of CCN number concentration. The non-hydrostatic, compressible version of RAMS is configured on an Arakawa-C grid and sigma-z terrain-following coordinate system (Cotton et al., 2003). For these simulations, the model uses two-way nesting with a nested 4-grid arrangement centered over Colorado. The outer grid-1 covers the continental United States with 60km grid spacing (62 x 50 grid pts), grid-2 covers Colorado and the adjacent surrounding states with 15km grid spacing (54 x 50 grid points), grid-3 encompasses much of Colorado with 3km grid spacing (97 x 82 grid points), and grid-4 covers the north-south oriented Park Range from the cities of Hayden to Walden with 750m grid spacing (114 x 114 grid points) (Fig. 1). Within each grid there are 40 vertical levels with a minimum of 75m grid spacing. The model uses vertical grid stretching with a stretch ratio of 1.12 and a maximum vertical grid spacing of 750m.

The RAMS model contains a highly sophisticated, state-of-the-art microphysics package that predicts on two-moments of the hydrometeor distributions (mixing ratio and number concentration) for rain, pristine ice, snow, aggregates, graupel, and hail (Walko et al., 1995; Meyers et al., 1997). Saleeby and Cotton (2004) extended the two-moment approach to the cloud droplet distribution via a parameterization for the formation of cloud droplets from activation of CCN and GCCN within a lifted parcel. The Lagrangian parcel model of Heymsfield and Sabin (1989), was utilized to determine the percent of user-specified CCN that would deliquesce, activate, and grow by condensation into cloud droplets for a given ambient temperature, vertical velocity, concentration of CCN, and median radius of the CCN distribution. The cloud droplet spectrum was

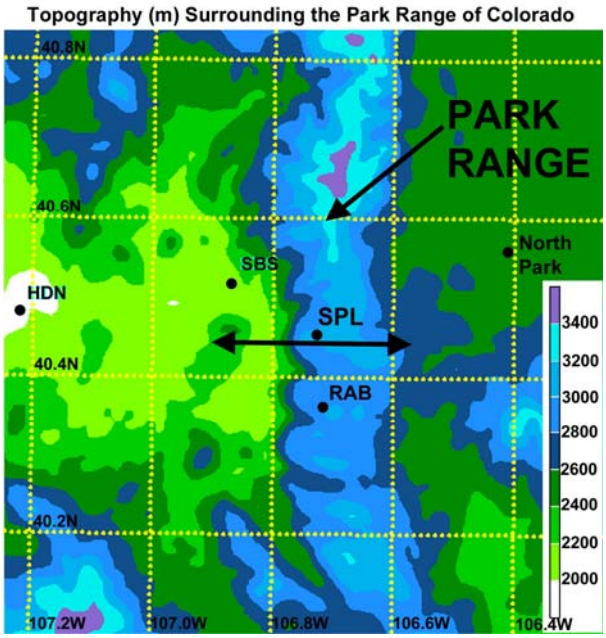

Figure 1. RAMS Grid-4 with grid spacing of 750m. Topography is overlaid (m). Locations of Hayden (HDN), Steamboat Springs (SBS), Storm Peak Lab (SPL), Rabbit Ears Pass (RAB), and North Park are labeled for reference. The bold-horizontal line depicts the cross-section range in figure 2.

further modified to behave as a bi-modal distribution with small cloud droplets (cloud1) from 2-40 μm in diameter and large cloud droplets (cloud2) from 40-80 μm in diameter. The parameterized activation of CCN (GCCN) and growth of their solution droplets results in direct formation of cloud1 (cloud2) droplets.

For this study we are only examining the impact of variable CCN concentrations. The CCN concentration was initialized horizontally homogeneous with a vertical profile that decreases linearly with height up to 4km AGL. Initial surface concentrations were varied from 100 – 1900 cm^{-3}; the minimum concentration allowed at any location was 100 cm^{-3}. The aerosol concentrations are represented by a polydisperse field on a lognormal distribution with a median radius for CCN of 0.04μm. As a simple source/sink function, CCN are depleted upon droplet nucleation and replenished upon droplet evaporation.

For these simulations, the 32km North American Regional Reanalysis was used for model initialization and nudging of the lateral boundaries. Each simulation began at 1200 UTC 7 February 2005 and was run for 36 hours for the duration of this snowfall episode.

3. OROGRAPHICALLY VARIED PRECIPITATION

a. Variability in orographic precipitation

All analyses discussed herein are results from the high resolution grid with 750m grid spacing. This fine resolution provides numerous grid point calculations along the sloping terrain to the west and east of SPL. The steepest terrain adjacent to SPL is the western

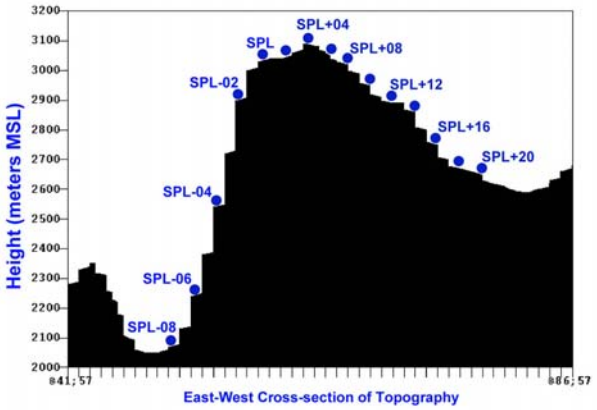

Figure 2. West to east model topographic cross-section centered roughly on SPL. Blue dots depict location of horizontal grid points, such that "SPL+04" is 4 model grid points east of SPL. Cross-section location is shown by the horizontal, bold, arrow-tipped line in figure 1.

slope that descends to the valley of the Steamboat Springs ski resort. The model contains 10 grid points at various elevations between SPL and the base of the ski resort. This allows for a high resolution look at the impact of orography on snowfall amounts as well as the influence of CCN concentration at various points along the terrain. Figure 2 provides a west to east cross-section of topography, centered on SPL, with reference locations labeled on the figure that will be pointed to in this paper.

Model predicted precipitation along the sloping terrain near SPL is shown figure 3. This figure also depicts the variation in precipitation between the cleanest case (CCN = 100 cm^{-3}) and most-polluted case (CCN = 1900 cm^{-3}). As a source of verification, the observed storm-total liquid equivalent precipitation, measured just upwind of SPL at the Steamboat patrol station headquarters (PHQ), was 23mm. The simulated totals near PHQ, from figure 3 point SPL-01, are in close agreement with this observation.

The most striking variability in precipitation is the rapid decrease in accumulation with decrease in elevation relative to the summit. The base of the slope to the west received only 1/6th the amount of precipitation of the summit. It is also interesting that the greatest precipitation occurred just downwind of SPL at grid point SPL+06. The model topography depicts the highest grid point as SPL+04; this may differ slightly from reality given that the assimilated topographic data has a resolution of 30 arc seconds, which is slightly coarser than the model grid spacing of 750m. Despite this difference, the greatest model predicted precipitation occurs downwind of the highest elevation, and not at the highest point itself.

The smallest accumulations shown here occur at the lower elevation areas of Hayden and North Park, which are well to the west and east of SPL, respectively. This certainly suggests that orographic influences were driving much of the precipitation from this winter system.

The impact of increasing CCN concentration from a clean to polluted type of environment can be assessed from a "total magnitude" and "relative

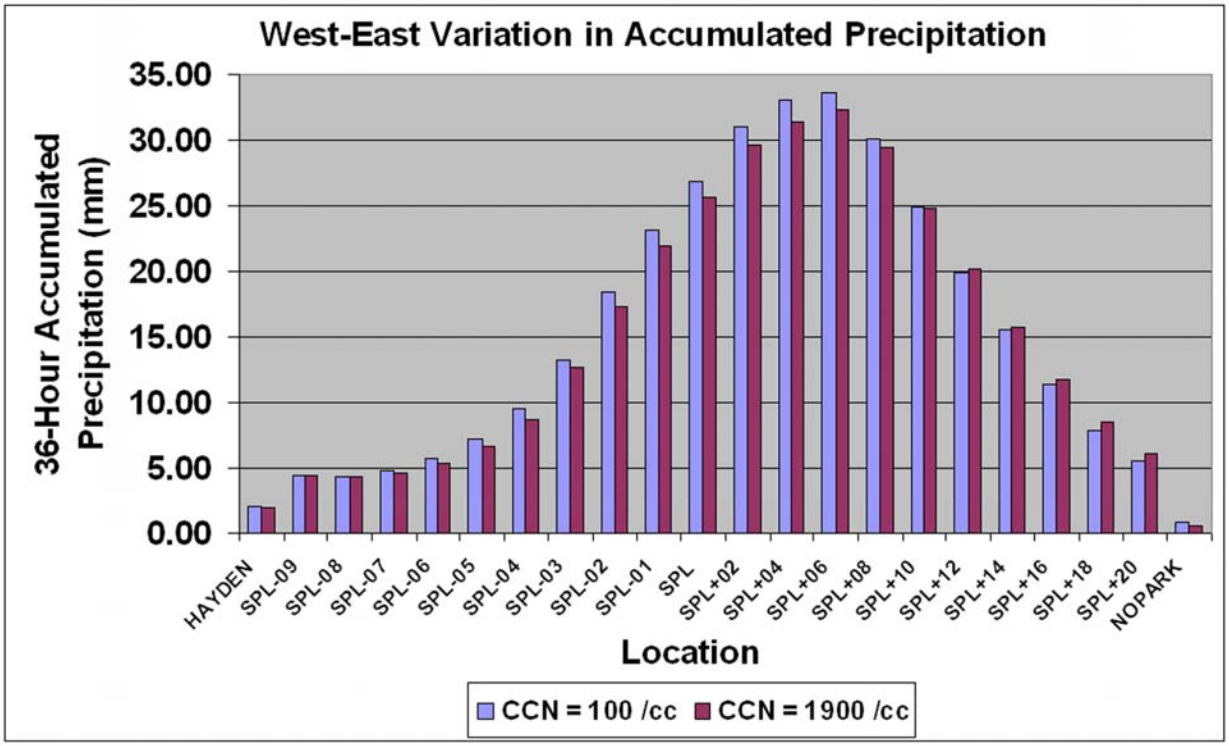

Figure 3. Accumulated precipitation for locations pointed to in figures 1 and 2. Graph also displays difference in accumulation between the cleanest (max CCN = 100 cm^{-3}) and most polluted (max CCN = 1900 cm^{-3}) case.

difference" type of viewpoint. An increase in CCN produces a decrease in accumulated precipitation of about 2mm along the summit area and western slope (~ 5% decrease at SPL+04). At the lower slope elevations, a decrease of 2mm represents a greater relative change. At the location of North Park, the precipitation amount decreased by 36% from 0.89mm to 0.57mm.

b. Cloud droplet properties

As mentioned earlier, an increase in aerosol concentration should lead to an increase in cloud droplet concentration and a decrease in droplet diameter. Figure 4 depicts the time evolution of droplet mixing ratio, number concentration, and mean diameter for the clean and polluted cases at the lowest model level closest to SPL. Periodic data from SPL is also overlaid for comparison. Droplet spectra data were available for this case from 2330UTC Feb 7 – 0545UTC Feb 8 and from 1300UTC Feb 8 – 2130UTC Feb 8.

The cloud mixing ratio time series remains generally consistent between the clean and polluted cases with greater differences seen in the latter half of the simulation. In a bulk sense, the average mixing ratio over the time period shown is greater for the polluted case (0.149 g kg^{-1}) than the clean case (0.139g kg^{-1}). This is likely due to reduced cloud water depletion by riming and/or increased droplet vapor depositional growth. An increase in the bulk vapor deposition in the polluted case is possible given the dramatic increase in number concentration of droplets. The polluted case provides a greater number of cloud droplet sites and surface area for vapor deposition. However, the polluted simulation is not representative of this case as seen in the time series of droplet concentration. The highest observed concentration for the limited observational data is just above 200 cm^{-3}. However, given the trend seen at the beginning of the observation period at SPL (~0.7 g m^{-3}, 190 cm^{-3}), it is likely that concentrations were well above 200 cm^{-3} prior to 2330 UTC Feb 7.

Given the relative consistency in mixing ratio between the clean and polluted cases, the large increase in droplet concentration for the polluted case must result in reduced droplet size. During times in which the simulated orographic cloud is present over SPL, the difference in mean droplet diameter between simulations is often greater than 10µm. In the polluted case the mean droplet diameter never exceeds 10µm, meaning that there are substantially more droplets in the distribution that do not reach the critical diameter, below which, riming nearly shuts off.

As expected, the observations tend to agree more closely to the clean case than the polluted case, with the clean case being a bit too pristine than reality. Past studies have shown that cloud droplet concentrations at SPL rarely exceed 400 cm^{-3} in the most polluted cases for that region (Borys et al., 2000; Borys et al. 2003; Lowenthal et al., 2002). However, given that anthropogenic emissions continue to increase, it is relevant to examine potential impacts of aerosol loading on precipitation and snowpack.

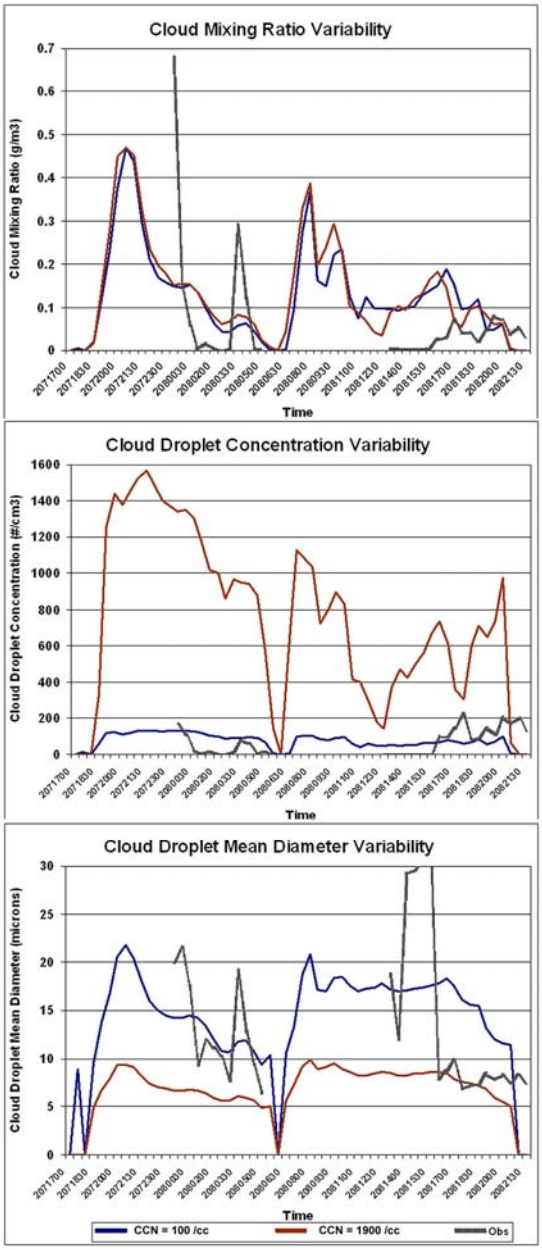

Figure 4. Time series of cloud mixing ratio (g m^{-3}, top), cloud droplet number concentration (cm^{-3}, middle), and droplet mean diameter (µm, bottom) at the closest grid point to SPL for the clean and polluted simulations. Available observations from SPL are overlaid as well.

c. Riming Impact on Ice Species Growth

Higher concentrations of CCN produce smaller cloud droplets which have a reduced riming efficiency by falling snow crystals. From Wang and Ji (2000), the riming efficiency between 1mm diameter broad-branched crystals and cloud droplets with diameters of 15µm and 30µm is approximately 0.20 and 0.65, respectively. Saleeby and Cotton (2006) have introduced these size-dependent riming efficiencies into RAMS in a newly developed binned approach to riming

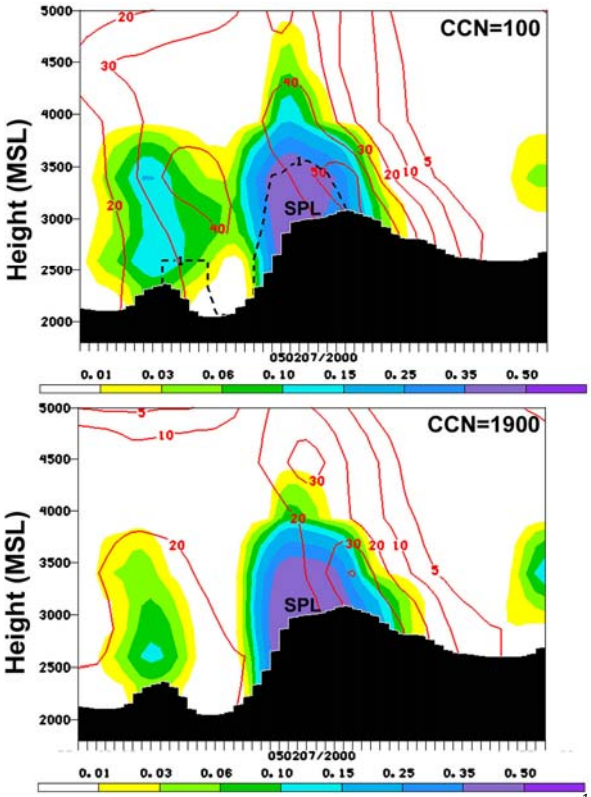

Figure 5. Cross-section of mixing ratio for cloud water (g kg^{-1}, shaded), aggregates (g kg^{-1} x 100, solid red lines), and graupel (g kg^{-1} x 100, black dashed lines). Top (bottom) panel is from the clean (polluted) simulation. SPL location is noted, and each tick mark is 750m. This chosen time contains the maximum cloud liquid water content.

of cloud droplets by the various ice species. This approach more accurately represents the riming process within RAMS' bulk microphysics framework. This is especially important when trying to best simulate the "seeder-feeder" process that occurs within the orographic cloud that envelops SPL during much of the winter. Each test simulation conducted here produced an ample orographic cloud over Mt. Werner. Figure 5 depicts hydrometeor mixing ratios along a cross-section, centered on SPL, at the time of highest simulated cloud liquid water for both the clean and polluted cases.

In these simulations, the orographic cloud reaches its greatest size and highest LWC near 2000 UTC Feb 7. The cloud is centered over SPL and extends about 5-6km east and west of SPL. Two importance differences between the clean and polluted simulations can be seen in figure 5. First, the aggregate mixing ratio is higher in the clean case within the region of the orographic cloud due to greater amounts of riming; coincident with this, the orographic cloud has reduced LWC in the areas of maximum aggregate mixing ratio. Secondly, only the clean simulation has any appreciable amount of graupel, which is co-located with the orographic cloud. The polluted case does not contain graupel because riming is reduced as a whole and because the rimed droplets are smaller. RAMS distinguishes graupel as a mixed phase hydrometeor.

Aggregates are composed of ice only, but graupel can be partly melted. When riming by aggregates occurs in the clean case, the rimed droplets are larger. Accretion of larger amounts of liquid causes the rimer to experience wet growth if the ambient temperature is not too low. Thus, the clean case produces heavier, wetter rime and allows for some graupel to be present. It should also be noted that graupel fall speeds are much more appreciable than snow or aggregates; this effect may also contribute to greater surface accumulation in the clean simulation.

d. Aerosol Impact on Rime and Precipitation Distribution

Given that rime has been shown to often comprise up to 50% of the total surface accumulated mass, the increase in pollution should reduce the amount of riming that occurs in the mountaintop orographic cloud. Figure 6a displays a time series of the volumetric sum of liquid cloud water (kg) removed by riming within the grid cell vertical column that encompasses SPL. From this, we see that the polluted case results in reduced riming above SPL throughout the duration of the simulation. To extend this look at riming beyond SPL, figure 6b displays the time series of the mass of cloud water that is rimed within the entire volume of Grid-4. On the whole of Grid-4, the amount of rimed cloud water is reduced in the polluted case at nearly all times for the duration of the simulation.

The reduction in riming due to higher CCN concentrations can explain the reduction in precipitation along the windward slopes within the area of the orographic cloud. However, along the lee slope to the east of SPL, we actually see several grid points (SPL+12 to SPL+20) in which the polluted case tended to produce an increase in surface accumulation (see figure 3). While this increase opposes the traditional tendency for precipitation suppression by pollution, it is certainly plausible that the upwind precipitation decrease is related to the downwind increase. If upwind riming is reduced, typical snow crystals and aggregates would likely have reduced sizes and slower fall speeds. In such a case, winds would tend to advect these hydrometeors further downstream before depositing at the surface.

To test this theory, the mean diameter of the distribution of aggregates was averaged every 30 minutes over the course of the simulation at both the SPL location and downwind at SPL+16. The aggregate hydrometeor category was analyzed here since this species comprises the majority of surface accumulation by at least an order of magnitude over pristine snow crystals. At the SPL grid location, the average aggregate mean diameter at 30m AGL decreased from 1.71mm to 1.68mm, and at 1000m AGL this was reduced from 1.40mm to 1.34mm. Thus, near the top and bottom of the orographic cloud over SPL, the aggregate fall speeds would be slower in the polluted case, which would allow greater downwind advection. At SPL+16, on the downwind slope, the aggregate mean diameters at 30m and 1000m AGL increased from 1.46mm to 1.48mm and 1.07mm to 1.08mm,

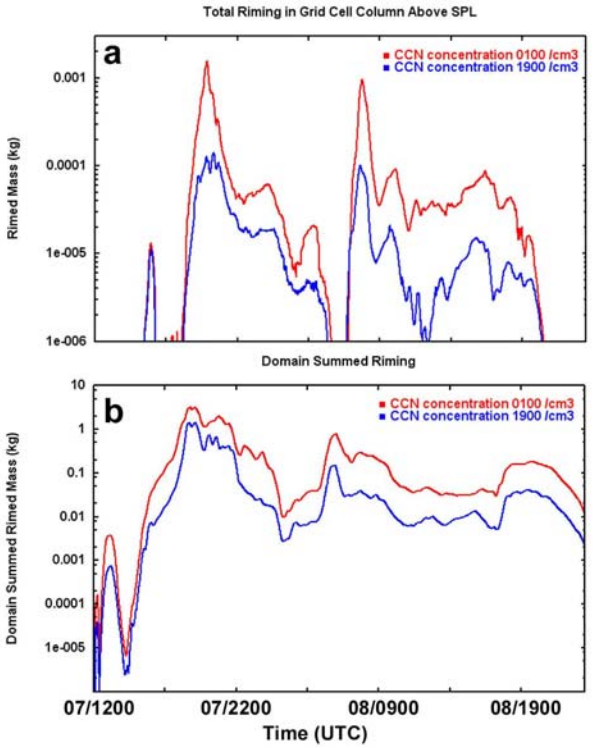

Figure 6. Time series of the mass of cloud water rimed (a) in the grid cell column above SPL and (b) within the entire 3D domain of grid-4. Red (blue) curve is for the simulation with initial maximum CCN concentration of 100 (1900) cm^{-3}.

respectively. So, when the CCN concentration is increased, (1) the riming rate is decreased, (2) the aggregates that initially advect into the windward slope orographic cloud grow more slowly, (3) these smaller aggregates have slower fall speeds and are subject to horizontal advection for a greater period of time, (4) and thus, the total accumulated snow amounts undergo a downwind translation.

4. CONCLUSIONS

The CSU-RAMS model has been utilized in the current study to investigate the impact of pollution aerosols on orographically enhanced wintertime precipitation. The nested, fine resolution grid with 750m grid spacing was focused over the north-south aligned Park Range of Colorado, extending from Hayden in the west toward North Park in the east. RAMS was chosen for this study because of its Lagrangian parcel model based parameterization for the activation of aerosols and nucleation of cloud droplets (Saleeby and Cotton, 2004), as well as its newly implemented binned scheme for simulating the riming growth process of frozen hydrometeors (Saleeby and Cotton, 2006).

In this study, a set of 36 hour simulations were run for a snowfall event occurring from 1200 UTC Feb 7 to 0000 UTC Feb 9, 2005. This event produced 35cm of new snow (23mm SWE) at the Steamboat Springs Ski Resort Patrol Station Headquarters (PHQ). RAMS was run for the duration of this case for varying profiles of CCN concentration from 100 to 1900 cm^{-3}. The

extremes of this range essentially represent a clean versus polluted type of environment.

Results have shown that the precipitation along the upwind slope leading to Mt. Werner was reduced in the highly polluted case. However, the leeward slope experienced an increase in precipitation, likely due to "blow-over" from the windward side of the mountain. During much of the simulation, Mt. Werner, including SPL and PHQ, was enveloped in an orographic cloud. Snow falling thru this cloud increases its overall mass via riming of cloud droplets. The droplet concentration and size impacts the degree of riming, and, thus, the snow crystal sizes. In the polluted case, with abundant CCN, the droplets are smaller and have lower riming efficiencies. This results in smaller snow crystals with slower fall speeds that are more likely to be transported further downwind before depositing at the surface.

The change in CCN concentration also impacts the relative predominance of various hydrometeor species and hydrometeor density. In the polluted case, where the orographic cloud droplets are smaller and riming is reduced, the rimed crystals are more likely to retain their primary crystal shape and density. In the cleaner case, where riming is greater and individual droplets contain more liquid water, the rimer particles may undergo wet growth. Thus, the clean case contains more graupel and less snow and aggregate mass. The fall speed of graupel and heavily rimed aggregates is greater than that for more pristine, lightly rimed crystals; thus deposition at the windward surface is greater.

Acknowledgements: This research was supported by the National Science Foundation under grant ATM-0451439 and by UCAR-NCAR-COMET under grant S04-44700. Logistical assistance from the Steamboat Ski and Resort Corporation is greatly appreciated. The Desert Research Institute is an equal opportunity service provider and employer and is a permittee of the Medicine-Bow and Routt National Forests.

5. REFERENCES

Borys, R.D. and M.A. Wetzel, 1997: Storm Peak Laboratory: A research, teaching, and service facility for the atmospheric sciences. *Bull. Am. Meteorol. Soc.*, **78**, 2115–2123.

_____, D.H. Lowenthal, and D.L. Mitchell, 2000: The relationships among cloud microphysics, chemistry, and precipitation rate in cold mountain clouds. *Atmos. Environ.*, **34**, 2593-2602.

_____, _____, S.A. Cohn, and W.O.J. Brown, 2003: Mountaintop and radar measurements of anthropogenic aerosol effects on snow growth and snowfall rate. *Geo. Res. Lett.*, **30**, 1538, doi:10.1029/2002GL016855.

Cotton, W. R., R. A. Pielke Sr., R. L. Walko, G. E. Liston, C. J. Tremback, H. Jiang, R. L. McAnelly, J. Y. Harrington, M. E. Nicholls, G. G. Carrio, and J. P. McFadden, 2003: RAMS 2001: Current status and future directions. *Meteorol. Atmos. Phys.*, **82**, 5-29.

Hindman, E.E., M.A. Campbell, and R.D. Borys, 1994: A ten-winter record of cloud-droplet physical and chemical properties at a mountaintop site in Colorado. *J. Appl. Meteor.*, **33**, 797-807.

Hindman, E.E., 1986: Characteristics of supercooled liquid water in clouds at mountaintops in the Colorado Rockies. *J. Clim. Appl. Meteor.*, **25**, 1271-1279.

Heymsfield, A. J., and R. M. Sabin, 1989: Cirrus crystal nucleation by homogeneous freezing of solution droplets. *J. Atmos. Sci.*, **46**, 2252-2264.

Lowenthal, D.H., R.D. Borys, and M.A. Wetzel, 2002: Aerosol distributions and cloud interactions at a mountaintop laboratory. *J. Geo. Res.*, **107**, 4345, doi:10.1029/2001JD002046.

Meyers, M.P., R.L. Walko, J.Y. Harrington, and W.R. Cotton, 1997: New RAMS cloud microphysics parameterization. Part II. The two-moment scheme. *Atmos. Res*. **45**, 3-39.

Mitchell, D.L., R. Zhang, and R.L. Pitter, 1990: Mass dimensional relationships for ice particles and the influence of riming on snowfall rates. *J. Appl. Meteor.*, **29**, 153-163.

Pruppacher, H., and J. Klett: 1997. Microphysics of Clouds and Precipitation. Second Revised Edition. Volume 18. Kluwer Academic Publishers. Dordrecht/Boston/London. Printed in The Netherlands.

Rauber, R.M., L.O. Grant, D. Feng, and J.B. Snider, 1986: The characteristics and distribution of cloud water over the mountains of northern Colorado during wintertime storms. Part I: Temporal variations. *J. Climate Appl. Meteor.*, **25**, 468-488.

Rauber, R.M., L.O. Grant, D. Feng, and J.B. Snider, 1986: The characteristics and distribution of cloud water over the mountains of northern Colorado during wintertime storms. Part II: Spatial distribution and microphysical characteristics. *J. Climate Appl. Meteor.*, **25**, 489-504.

Reinking, R.F., J. B. Snider, and J.L. Coen, 2000: Influences of storm-embedded orographic gravity waves on cloud liquid water and precipitation. *J. Appl. Meteor.*, **39**, 733–759.

Saleeby, S.M., and W.R. Cotton, 2004: A large droplet mode and prognostic number concentration of cloud droplets in the Colorado State University Regional Atmospheric Modeling System (RAMS). Part I: Module descriptions and supercell test simulations. *J. Appl. Meteor.*, **43**, 182-195.

_____, and _____, 2006: A binned approach to cloud droplet riming implement in a bulk microphysics model. *J. Appl. Meteor.*, In preparation**.**

Walko, R.L., W.R. Cotton, M.P. Meyers, and J.Y. Harrington, 1995: New RAMS cloud microphysics parameterization: Part I. The single-moment scheme. *Atmos. Res.*, **38**, 29-62.